A Hydrophobic Gating Mechanism for Nanopores

Oliver Beckstein, Philip C. Biggin, and Mark S. P. Sansom*

Laboratory of Molecular Biophysics, Biochemistry Department, University of Oxford, South Parks Road, Oxford, OX1 3QU, U.K.

Received: June 13, 2001; In Final Form: October 19, 2001

Water-filled pores of nanometer dimensions play important roles in chemistry and biology, e.g., as channels through biological membranes. Biological nanopores are frequently gated, i.e., they switch between an open and a closed state. In several ion channel structures the gate is formed by a ring of hydrophobic side chains that do not physically occlude the pore. Here we investigate whether a hydrophobic pore can act as a gate via molecular dynamics simulations of the passage of water through atomistic models of nanopores embedded within a membrane mimetic. Both the geometry of a nanopore and the hydrophilicity vs hydrophobicity of its lining determine whether water enters the channel. For purely hydrophobic pores there is an abrupt transition from a closed state (no water in the pore cavity) to an open state (cavity water at approximately bulk density) once a critical pore radius is exceeded. This critical radius depends on the length of the pore and the radius of the mouth region. Furthermore, a closed hydrophobic nanopore can be opened by adding dipoles to its lining.

Introduction

Water-filled pores of nanometer dimensions are of importance in chemistry [1,2] and biology,[3,4] e.g., as channels through biological membranes. A biological channel consists of a pore ca. 3 nm long that spans a lipid bilayer membrane. Channels are usually "gated", i.e., they contain a region that can interrupt the flow of molecules (water, ions) that is often coupled to a sensor that controls the gate allosterically. The question of how gating works at an atomic level is one of considerable complexity. A pattern is emerging for some channels (e.g., the nicotinic acetylcholine receptor,[5,6] bacterial potassium,[7,8] and bacterial mechanosenitive [9,10] channels) in which the most constricted region of the pore (which is usually identified with the gate) is ringed by hydrophobic amino acid side chains, e.g., leucine or valine. For the nicotinic acetylcholine receptor, even when this channel is functionally closed the pore appears to be physically open, with a radius of about 3.5 Å,[5,6] leaving enough space to accommodate up to three water molecules. So, is an effect other than steric occlusion able to close a channel, i.e., hydrophobic gating? Experimental evidence in favor of such a mechanism comes from studies of pores in modified Vycor glass (radius ca. 30 Å), which showed that water failed to penetrate these pores once a threshold hydrophobicity of the pore walls was exceeded.[11] However, it is unclear whether these results can be transferred directly to biological systems.

Several simulation studies have focused on water and/or ions in model nanopores.[12−16] Our model (Figure 1) contains some important novel features. It is a membrane-spanning channel of finite length, rather than an infinite [13,14] or closed [17] cylinder as in some previous investigations of water in nanopores. Because our model allows water molecules within the pore to equilibrate with those in the bulk phase, it avoids any prior assumptions about water density. Thus, effectively, the interior of the pore is simulated in a grand canonical ensemble. Also, our model is rough on an atomic scale. The pseudoatoms forming the pore are not fixed but can vibrate about their equilibrium positions, thus mimicking the flexibility of a real channel protein. Thus we are able to probe entry/exit of water to/from an atomistic model of a nanopore, while retaining control over its geometry and the charge pattern of its pore lining.

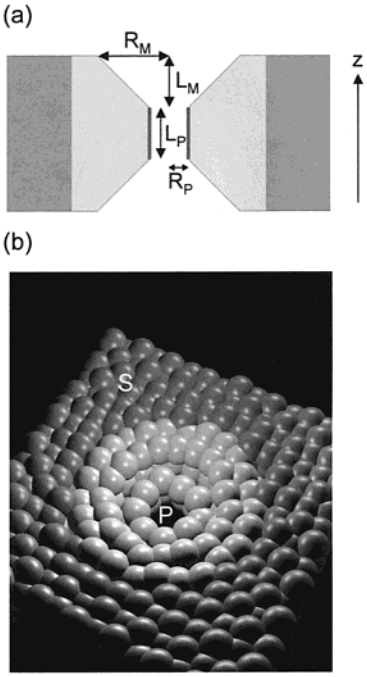

Figure 1. (A) Pore model, in cross-section along the pore axis (z), defining the pore radius (R_P), the mouth radius (R_M), and the pore length (L_P). During the simulations, the following parameter ranges were explored: $R_P = 3.5$ to 11 Å; $R_M = 7.5$, 10, 18 Å, and no mouth region; and $L_P = 8$ and 12 Å. The mouth length was fixed at $L_M = 4$ Å throughout, other than in the no mouth, i.e., $L_M = 0$, simulation. The thickness of the bilayer mimetic slab is chosen as $d_{SLAB} = 2L_M + L_P + 1$ Å. (B) van der Waals surface of a pore model (P) embedded in a membrane-mimetic slab (S) (diagram prepared with VMD v1.6 [30]).

Methods

Model. A cylindrical hydrophobic nanopore of pseudoatoms surrounds a cavity that opens toward the bulk volume at both

* To whom correspondence should be addressed: e-mail mark@biop.ox.ac.uk; phone +44-1865-275371; fax +44−1865−275182

10.1021/jp012233y CCC: $20.00
Published on Web 12/05/2001

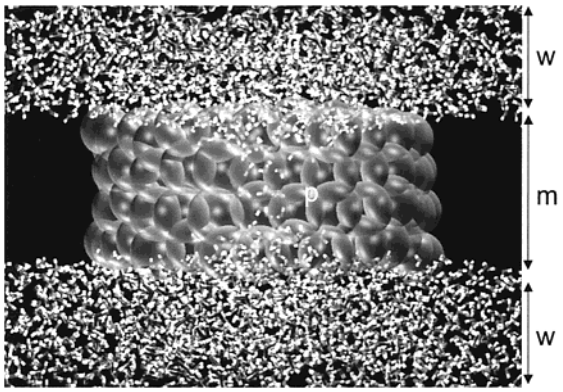

Figure 2. Snapshot from a simulation with a hydrophilic pore lining (i.e., a dipole present) showing the water molecules (w; stick format) and the pore (p) atoms (as van der Waals spheres). The "membrane" (m) is omitted for clarity.

ends in a funnel shape, thus creating two symmetric mouth regions. This pore is embedded in a slab of pseudoatoms that mimics a membrane (Figure 2). The pseudoatoms have the characteristics of methane molecules, i.e., they are uncharged with a van der Waals radius of 1.95 Å. Each pseudoatom was held at its initial position by a restraining force ($k = 100$ kJ mol $^{-1}$ Å^{-1}).

To generate hydrophilic pores, different numbers of pseudoatoms had partial charges placed on them. A dipole moment of 2×10^{-29} Cm was created by placing partial charges of ± 0.38 e (the charge on a peptide backbone carbonyl oxygen in the GROMOS96[18] force field) on adjacent pseudoatoms, such that the dipole moment lies parallel to the pore (z) axis.

Simulation Details. Molecular dynamics (MD) simulations were performed with GROMACS v2.0,[19] using a 2 fs time step and saving coordinates every 0.5 ps. The nanopore model embedded in the slab was solvated in a box of preequilibrated SPC[20,18] water so that there was 15 Å of bulk-like water on each side of the membrane. Simulations were at constant particle number and temperature (300 K), using a Berendsen thermostat,[21] with a time constant of 0.1 ps. Weak pressure coupling (compressibility 4.5×10^{-5} bar^{-1}, time constant 1 ps) was employed for the z dimension, while the x and y dimensions of the simulation box were held fixed at 60 Å. Long-range electrostatic interactions were computed with a particle mesh Ewald method[22] (cutoff = 1 nm; grid width = 0.15 nm; and 4th order interpolation), using periodic boundary conditions.

Analysis. We measure the time-dependent openness, ω, of a pore in terms of the density of water within the pore relative to that of bulk water. A pore is said to be in the open state if water penetrates and consequently the density is larger than a threshold of 0.5 g cm^{-3} (i.e., half the density of bulk water) and we assign $\omega = 1$. Otherwise it is closed ($\omega = 0$). Trial calculations suggest that our results are insensitive to the exact value of the threshold. The average openness over a simulation is $\langle\omega\rangle = T_{open}/T_{simulation}$, i.e., the fraction of the simulation time during which the channel is in an open state. The water density is calculated from the accessible volume of the cylindrical pore as obtained from a corrected radius $R^* = R - 0.81$ Å, where R is the hard sphere radius of the pore-lining pseudoatoms. The correction to R takes into account the van der Waals radii of methane and water molecules and their intermolecular van der Waals distance (i.e., the minimum in the water−methane interaction potential).

TABLE 1: Geometrical Parameters and Patterns of Partial Charges for Nanopore Models[a]

L_M	R_M	L_P	R_P	charge pattern
0	-	8	3 to 8	0, (D1)
4	7.5	8	3.5 to 7.5	0
	10	8	3.5 to 10	0, D1, D2, (D6)
		12	3.5; 7 to 8	0, D2
	18	8	3.5 to 7.5	0, D2, (D2a, D4, Q2)
		12	5,6; 3.5	0, D2

[a] Geometrical parameters are defined in Figure 1. All distances are in Å. Charge patterns are: 0 − only hydrophobic pseudo atoms; D1 − single dipole parallel to the pore (charges +0.38 e and −0.38 e); DN − N parallel dipoles; D2a − two antiparallel dipoles; Q2 − two quadrupoles. (Those patterns in parentheses indicate that only selected geometries in a given range were calculated for this charge pattern.)

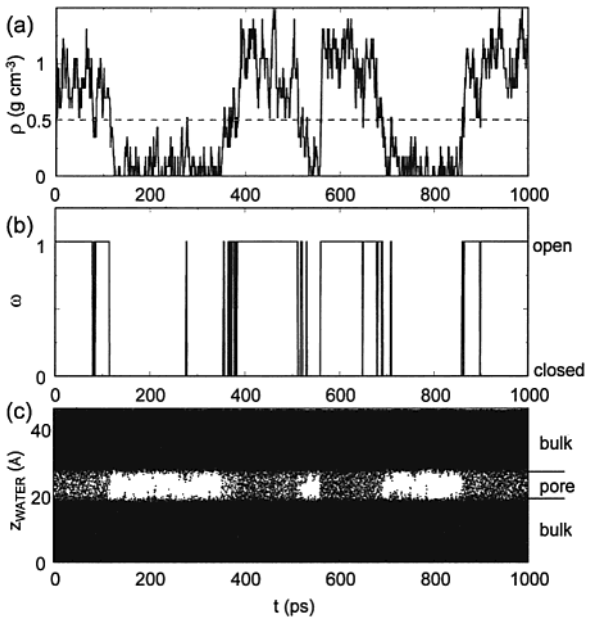

Figure 3. Channel water density ρ (A) and openness ω (B) for a 1 ns simulation of an electroneutral ($q = 0$) pore with $R_M = 18$ Å, $R_P = 4.5$ Å, and $L_P = 8$ Å. If $\rho < 0.5$ g cm^{-3} (broken horizontal line in (a)) then the channel is closed ($\omega = 0$); if r ≥ 0.5 g cm^{-3}, then the channel is open ($\omega = 1$). For this simulation the average openness is $\langle\omega\rangle = 0.53$. (C) Visualization of water positions along the pore (z) axis vs time for the same simulation. Each dark point represents the center of mass of a water molecule.

Results and Discussion

A number of simulations (typically of duration 1 ns; see Table 1) have been run in which pore geometry and pore lining charge pattern have been varied in order to determine the influence of these parameters on ω. Hydrophobic pores remain closed (i.e., water fails to penetrate) if the pore radius is less than ca. 4.5 Å. For a given pore length and mouth radius there is a critical transition radius above which the channel is constitutively open. Examination of ω vs time for a channel close to the transition radius reveals that the channel fluctuates on a ca. 100 ps time scale between an open and a closed state (Figure 3a,b). It is tempting to compare this with the gating kinetics of real ion channels.[23,24] At a microscopic level, these fluctuations in the degree of openness correspond to formation/destruction of a continuous column of water molecules within the pore (Figure 3c).

For purely hydrophobic pores gating depends on both the pore radius R_P and the mouth radius R_M (Figure 4). The channel is constitutively closed at small pore radii (<4.5 Å) and also at small mouth radii (7.5 Å). For all mouth radii channels are

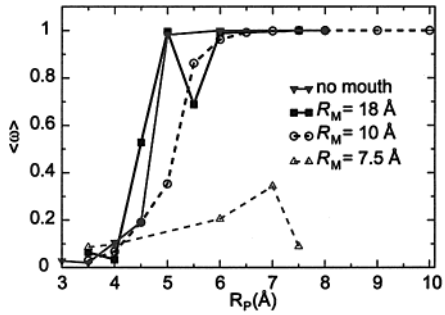

Figure 4. Average degree of openness $<\omega>$ vs pore radius R_P for hydrophobic pores with various mouth radii, R_M. Simulation times are 1 ns per point. For the smallest mouth radius the channel does not fully open, even at high R_P values. As the mouth radius is increased the critical pore radius above which the channel is open decreases. For $R_M = 10$ Å a typical set of data points is plotted, each value is close to the average of 5 to 9 independent 1 ns simulations (see Figure 7).

closed if $R_P = 3.5$ Å, even though three water molecules could fit in such a pore on purely geometrical criteria. For $R_M = 10$ Å (n.b. the absence of a mouth is considered as an infinitely wide mouth) then there is a transition between closed and open as R_P is increased. For $R_M = 10$ Å this transition occurs at R_P ~5 Å; for the other mouth radii the transition radius is at R_P ~4 Å. With increasing pore length (from 8 to 12 Å; see Table 1) the transition pore radius also increases. For example, for $R_P = 7$ and 10 Å, the channel is fully open if the length of the pore $L_P = 8$ Å but fully closed if $L_P = 12$ Å. Overall, a hydrophobic pore can be switched from closed to open by increasing its radius by as little as 1 Å. Note that in these simulations the pseudoatoms were not fixed but restrained, resulting in positional RMSDs (averaged over all pore atoms and over the total simulation time) ranging from 0.7 Å for narrow pores to 1.0 Å for wide pores. These should be compared with, e.g., RMSDs of ca. 1 Å for the side chain atoms of the gate region of KcsA in MD simulations.[25]

Increasing the hydrophilic character of the pore can also open a small radius pore (Figure 5). There is a weak dependence on the charge pattern. For example, for the $R_M = 18$ Å pore at a pore radius of 4 Å, two parallel dipoles (each of magnitude 2×10^{-29} Cm) have a greater effect in increasing ω than do two antiparallel dipoles. Even for the smallest radius pore considered ($R_P = 3.5$ Å), a pair of dipoles is above the threshold surface charge needed to open the $R_M = 18$ Å channel. We note that a peptide bond has a dipole moment[26] of ca. 1.2×10^{-29} Cm. Thus a closed hydrophobic channel can be opened by a modest increase in the surface charge density of the pore lining.

An interesting anomaly occurs for the $R_M = 10$ Å channel (Figure 5b) at $R_P = 3.5$ Å, for which a single dipole of 2×10^{-29} Cm is sufficient to fully switch the channel from closed to open, even though the $R_P = 4$ Å pore remains closed in response to the same single dipole. Thus, the $R_P = 3.5$ Å channel seems to be the exception to the requirement for at least two dipoles to open the channel at narrow radii. This may correlate with observations of anomalous diffusional behavior of water within infinitely long hydrophobic channels of radius ca. 4 Å,[13,14] which suggest that water structure at about this radius is anomalously stable. Thus, anomalous stability of water in such narrow pores may favor the open channel state. At $R_P = 3.5$ Å water formed disk-like layers along the length of the pore (Figure 6), similar to those seen in earlier simulations[13,14] of infinite channels. Typically, each disk contained four or five water molecules. The disks are not fixed relative to the pore, moving along its length on a ca. 0.2 ns time scale. Thus we are reasonably confident that they do not simply reflect the detailed

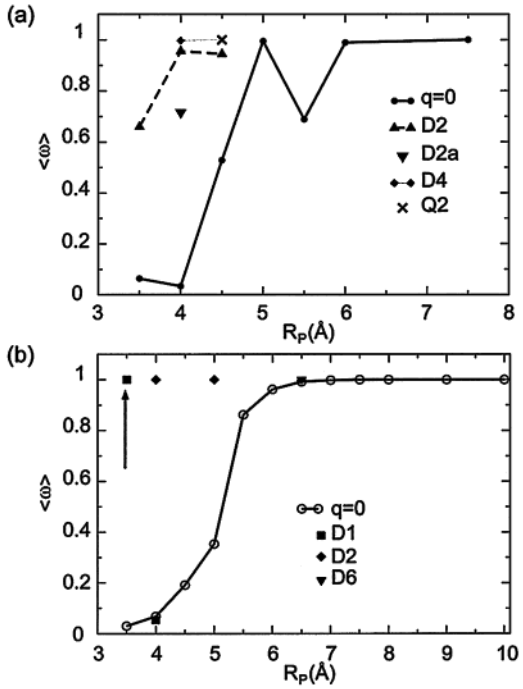

Figure 5. Average degree of openness vs pore radius for pores with various partial charges patterns (see Table 1). (A) $R_M = 18$ Å and $L_P = 8$ Å; (B) $R_M = 10$ Å and $L_P = 8$ Å. Simulation times are 1 ns per point. The arrow indicates anomalous behavior of the $R_P = 3.5$ Å pore with a single dipole of magnitude 2×10^{-29} Cm, oriented parallel to the pore axis.

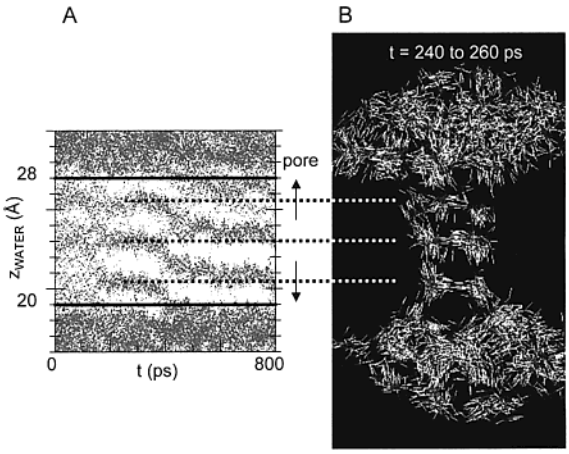

Figure 6. (A) Water positions (dark dots) along the pore (z) axis vs time for the $R_M = 10$ Å, $R_P = 3.5$ Å, D1 simulation. Layers of waters are evident. (B) Snapshots (superimposed) of waters within the pore at times between 240 and 260 ps. The broken lines indicate the approximate locations of the three "rings" of water molecules seen in this pore.

shape of the pore, but are a consequence of the preferred packing of water within this confined volume.

We have attempted to analyze possible errors arising from the use of relatively short (1 ns) simulations. For this we repeated the $R_M = 10$ Å and $L_P = 8$ Å simulations, to give between 5 and 9 simulations for each pore radius, each repeat simulation of 1 ns duration, but with different random seeds for the initial generation of velocities (corresponding to a Maxwell distribution at 300 K). The results (Figure 7) show that at low (less than 0.1) or high (ca. 1) values of the openness (ω) the standard deviation is relatively small. However, for intermediate values the standard deviation is greater. Careful inspection of the data (Figure 7) shows that for the intermediate

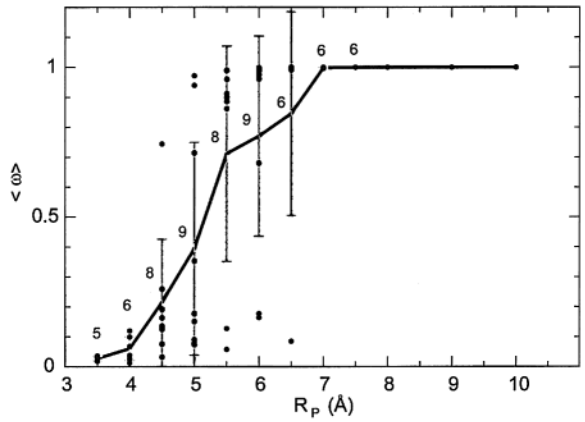

Figure 7. Average degree of openness vs pore radius for $R_M = 10$ Å and $L_P = 8$ Å pores, showing the variation between multiple simulations. Each point corresponds to a single 1 ns simulation. The solid curve is the average and the error bars are standard deviations. The numbers above the curve indicate the number of repeat simulations for each pore radius (where no number is given only a single simulation was run).

openness pore radii, in many cases there is a clear cluster of points with just one or two outlying simulations. For example, at $R_P = 6.5$ Å, of the six repeat simulations, five gave ω ca. 1 and only one simulation gave ω ca. 0.1. Thus we are reasonably confident that the overall trends discussed in this study are robust to variations due to the duration of the simulations.

Conclusions

In summary, hydrophobicity per se can close a sterically open channel to penetration by water and hence, by simple extension, to ions and small polar solutes. Such a channel can be opened by adding a relatively small number of dipoles to the lining of the pore or by a modest increase in radius. We note that, for example, the narrow central region of the aquaporin[3,4] pore has two dipolar asparagine residues present in an otherwise relatively hydrophobic pore lining. The critical gating radius depends on the geometry of the mouth region of the pore, a factor of 10 neglected. Simulation studies of gramicidin[27] suggested that 87% of overall channel resistance to water permeation comes from the energetic cost for a bulk water to enter the mouth. Thus, both overall dimensions and the extents of hydrophobic and hydrophilic regions in the lining provide a key to gating of nanopores.

The time dependent fluctuations in water density within a pore seen for "transitional" radii (see, e.g., Figure 3) are of interest. In long (>50 ns) simulations of water in a carbon nanotube, Hummer[16] observes water flux through the pore to occur in a pulsatory fashion, with fluctuations in flux on a time scale of ca. 4 ns. Thus, it may be a general property of water permeable pores that the water density within such pores fluctuates. We have seen further evidence for such fluctuations in simulations of the aquaporin protein GlpF.[28] Furthermore, recent theoretical studies have emphasized the relationship of fluctuations in number of particles within a pore to the geometry of that pore.[29]

Acknowledgment. This work was supported by grants (to M.S.P.S., to P.C.B. and to O.B.) from the Wellcome Trust.

References and Notes

(1) Gallo, P.; Rovere, M.; Spohr, E. *J. Chem. Phys.* **2000**, *113*, 11324.
(2) Gordillo, M. C.; Marti, J. *Chem. Phys. Lett.* **2000**, *329*, 341.
(3) Murata, K.; Mitsuoaka, K.; Hirai, T.; Walz, T.; Agre, P.; Heymann, J. B.; Engel, A.; Fujiyoshi, Y. *Nature* **2000**, *407*, 599.
(4) Ren, G.; Reddy, V. S.; Cheng, A.; Melnyk, P.; Mitra, A. K. *Proc. Natl. Acad. Sci. U.S.A.* **2001**, *98*, 1398.
(5) Unwin, N. *Nature* **1995**, *373*, 37.
(6) Unwin, N. *Philos. Trans. R. Soc. London B* **2000**, *355*, 1813.
(7) Doyle, D. A.; Cabral, J. M.; Pfuetzner, R. A.; Kuo, A.; Gulbis, J. M.; Cohen, S. L.; Cahit, B. T.; MacKinnon, R. *Science* **1998**, *280*, 69.
(8) Perozo, E.; Cortes, D. M.; Cuello, L. G. *Science* **1999**, *285*, 73.
(9) Chang, G.; Spencer, R. H.; Lee, A. T.; Barclay, M. T.; Rees, D. C. *Science* **1998**, *282*, 2220.
(10) Sukharev, S.; Betanzos, M.; Chiang, C. S.; Guy, H. R. *Nature* **2001**, *409*, 720.
(11) Hirama, Y.; Takahashi, T.; Hino, M.; Sato, T. *J. Colloid Interface Sci.* **1996**, *184*, 349.
(12) Partenskii, M. B.; Jordan, P. C. *J. Phys. Chem.* **1992**, *96*, 3906.
(13) Lynden-Bell, R.; Rasaiah, J. C. *J. Chem. Phys.* **1996**, *105*, 9266.
(14) Allen, T. W.; Kuyucak, S.; Chung, S. H. *J. Chem. Phys.* **1999**, *111*, 7985.
(15) Goulding, D.; Hansen, J.-P.; Melchionna, S. *Phys. Rev. Lett.* **2000**, *85*, 1132.
(16) Hummer, G.; Rasaiah, J. C.; Noworyta, J. P. *Nature* **2001**, *414*, 188.
(17) Sansom, M. S. P.; Kerr, I. D.; Breed, J.; Sankararamakrishnan, R. *Biophys. J.* **1996**, *70*, 693.
(18) van Gunsteren, W. F.; Kruger, P.; Billeter, S. R.; Mark, A. E.; Eising, A. A.; Scott, W. R. P.; Huneberger, P. H.; Tironi, I. G. *Biomolecular Simulation: The GROMOS96 Manual and User Guide*; Biomos & Hochschulverlag AG an der ETH Zurich: Groningen & Zurich, 1996.
(19) Berendsen, H. J. C.; van der Spoel, D.; van Drunen, R. *Comput. Phys. Comm.* **1995**, *95*, 43.
(20) Hermans, J.; Berendsen, H. J. C.; van Gunsteren, W. F.; Postma, J. P. M. *Biopolymers* **1984**, *23*, 1513.
(21) Berendsen, H. J. C.; Postma, J. P. M.; van Gunsteren, W. F.; DiNola, A.; Haak, J. R. *J. Chem. Phys.* **1984**, *81*, 3684.
(22) Darden, T.; York, D.; Pedersen, L. *J. Chem. Phys.* **1993**, *98*, 10089.
(23) Colquhoun, D.; Hawkes, A. G. *Philos. Trans. R. Soc. London B* **1982**, *300*, 1.
(24) Hille, B. *Ionic Channels of Excitable Membranes*, 2nd ed.; Sinauer Associates Inc.: Sunderland, Mass., 1992.
(25) Bernèche, S.; Roux, B. *Biophys. J.* **2000**, *78*, 2900.
(26) Hol, W. G. J.; van Duijnen, P. T.; Berendsen, H. J. C. *Nature* **1978**, *273*, 443.
(27) Chiu, S. W.; Subramaniam, S.; Jakobsson, E. *Biophys. J.* **1999**, *76*, 1939.
(28) Sansom, M. S. P.; Bond, P.; Beckstein, O.; Biggin, P. C.; Faraldo-Gómez, J.; Law, R. J.; Patargias, G.; Tieleman, D. P. *Novartis Foundation Symposia* **2002**, *245*, in press.
(29) Bezrukov, S. M.; Berezhkovskii, A. M.; Pustovoit, M. A.; Szabo, A. *J. Chem. Phys.* **2000**, *113*, 8206.
(30) Humphrey, W.; Dalke, A.; Schulten, K. *J. Mol. Graph.* **1996**, *14*, 33.